Targeted Disruption of the Protein Tyrosine Phosphatase-Like Molecule IA-2 Results in Alterations in Glucose Tolerance Tests and Insulin Secretion

Keiichi Saeki,[1] Min Zhu,[2] Atsutaka Kubosaki,[1] Jingping Xie,[1] Michael S. Lan,[2] and Abner Louis Notkins[1]

IA-2 is a major autoantigen in type 1 diabetes. Autoantibodies to IA-2 appear years before the development of clinical disease and are being widely used as predictive markers to identify individuals at risk for developing type 1 diabetes. IA-2 is an enzymatically inactive member of the transmembrane protein tyrosine phosphatase family and is an integral component of secretory granules in neuroendocrine cells. To study its function, we generated IA-2–deficient mice. Northern and Western blot analysis showed that neither IA-2 mRNA nor protein was expressed. Physical examination of the IA-2$^{-/-}$ animals and histological examination of tissues failed to reveal any abnormalities. Nonfasting blood glucose levels, measured over 6 months, were slightly elevated in male IA-2$^{-/-}$ as compared to IA-2$^{+/+}$ littermates, but remained within the nondiabetic range. Glucose tolerance tests, however, revealed statistically significant elevation of glucose in both male and female IA-2$^{-/-}$ mice and depressed insulin release. In vitro glucose stimulation of isolated islets showed that male and female mice carrying the disrupted gene released 48% ($P < 0.001$) and 42% ($P < 0.01$) less insulin, respectively, than mice carrying the wild-type gene. We concluded that IA-2 is involved in glucose-stimulated insulin secretion. *Diabetes* 51:1842–1850, 2002

IA-2 is a major autoantigen in type 1 diabetes (1,2). At the time of diagnosis, ~70% of newly diagnosed patients have autoantibodies to IA-2. Because these autoantibodies appear months and years before the onset of clinical symptoms, they have become useful markers for identifying individuals who are at high risk for developing type 1 diabetes (3–7). Individuals with no clinical symptoms, but who have autoantibodies to IA-2 and GAD, have an ~50% risk of developing type 1 diabetes within 5 years and an even higher risk within 7–10 years. For these reasons, the measurement of autoantibodies to recombinant IA-2 and GAD is being widely used to predict risk for type 1 diabetes (8,9).

IA-2 is a 979–amino acid transmembrane protein. It has an extracellular, transmembrane, and intracellular domain consisting of 576, 24, and 379 amino acids, respectively (1). Autoantibodies to IA-2 are directed exclusively to the intracellular domain, primarily to the COOH-terminus and, to a somewhat lesser extent, to the juxtamembrane region (10–12). The gene encoding IA-2 is located on human chromosome 2q35. The coding region extends over ~20 kb and consists of 23 exons (13). Exons 1–12 encode the extracellular domain; exon 13, the transmembrane domain; and exons 14 through 23, the intracellular domain. A region extending ~200 bp 5′-upstream from the translation start site and a region encompassing exon 1 and intron 1 have been shown to have strong promoter activity (R. Alam and A.L.N., unpublished data; 13).

The function of IA-2 is not known. Based on sequence analysis, IA-2 belongs to a subgroup of the transmembrane protein tyrosine phosphatase (PTP) family. Homologs have been found in cows, rats, mice, macaca, zebrafish, *Drosophilia*, and *Caenorhabditis elegans* and show 99, 98, 97, 73, 82, 58, and 46% identity, respectively, to human IA-2 (14). IA-2 differs from other PTPs in that it is enzymatically inactive because of substitution of amino acids (Ala 911→Asp and Asp 877→Ala) at conserved sites known to be critical for enzymatic activity (15). Electron microscopic studies and immunohistochemical studies have localized the IA-2 protein (also known as ICA512) to the secretory vesicles of neuroendocrine cells (16).

The present study was initiated to determine the function of IA-2 by targeted disruption of the mouse IA-2 gene. Mouse IA-2 is very similar to human IA-2. It is 981 amino acids in length, consists of 23 exons, and is located on mouse chromosome 1 (17). A targeting construct, in which the 5′-upstream promoter region, exons 1–3 and introns 1, 2, and most of 3, were replaced with a neomycin cassette, was used to transfect embryonic stem (ES) cells by homologous recombination. ES cells in which the IA-2 construct had become integrated were injected into blastocysts, and the resulting chimeric animals and their offspring were bred and tested for evidence of homologous recombination and germ-line transmission. Here we describe the successful targeted disruption of the IA-2 gene in mice and provide a description of the resulting phenotype.

From the [1]Experimental Medicine Section, Oral Infection and Immunity Branch, National Institute of Dental and Craniofacial Research, National Institutes of Health, Bethesda, Maryland; and the [2]Research Institute for Children, Children's Hospital, and Departments of Pediatrics and Genetics, Louisiana State University Health Sciences Center, New Orleans, Louisiana.

Address correspondence and reprint requests to Abner L. Notkins, National Institutes of Health, Building 30/Room 121, 30 Convent Dr., MSC 4322, Bethesda, MD 20892-4322. E-mail: anotkins@dir.nidcr.nih.gov.

Received for publication 30 November 2001 and accepted in revised form 11 February 2002.

K.S., M.Z., and A.K. contributed equally to the work.

ELISA, enzyme-linked immunosorbent assay; ES, embryonic stem; KRBB, Krebs-Ringer bicarbonate buffer; PTP, protein tyrosine phosphatase.

RESEARCH DESIGN AND METHODS

Generation of IA-2−deficient mice. A 129SvJ mouse genomic library (Stratagene, Cedar Creek, TX) was screened with a mouse IA-2 cDNA probe. A 17-kb fragment of mouse IA-2 containing the coding sequence of exons 1–13 was used to construct a targeting vector. A 3.5-kb *Sal*I-*Eco*RI fragment upstream of the first exon was subcloned into pBluescript SK+ (Stratagene). From this plasmid, the 5′-segment was subcloned as a 3.5-kb *Kpn*I-*Bam*HI fragment into pPNT vector (18), resulting in pPNT-5′IA-2. Subsequently, a 3.3-kb *Xho*I-*Xho*I fragment containing exons 4–6 was subcloned into pPNT-5′IA-2 vector, resulting in pPNT-IA-2. Homologous recombination resulted in the replacement of IA-2 exons 1–3 and introns 1, 2, and most of 3 with the neo-resistant gene cassette from the pPNT-IA-2 vector into the *Eco*RI-*Xho*I site of the targeted locus. The targeting plasmid was linearized using the unique *Not*I site before electroporation. The HSV-tk cassette was used for negative selection.

Jl ES cells (19) were transfected with the linearized targeting vector (50 μg/1.5 × 10^7 cells) using a BioRad Gene Pulser and grown under double-selection conditions (350 μg/ml G418, 2 μmol/l ganciclovir). After 7–10 days, G418-ganciclovir–resistant ES cell clones were picked and expanded (20).

Genomic DNA from individual ES cell clones was extracted and analyzed by Southern blot hybridization. A 1.1-kb *Xho*I-*Hin*dIII fragment (outside probe) containing exons 7 and 8 just downstream of the *Xho*I-*Xho*I segment was used for screening. Homologous recombinant clones selected by the outside probe were also analyzed with a 1.9-kb neo cassette probe to check for multiple integrations. Five ES cell clones were injected into C57BL/6 mice blastocysts to generate chimeras. Overt chimeras were backcrossed with C57BL/6 mice to produce germline transmission of the targeted allele. Tail DNA of agouti offspring and subsequent pups was screened for the presence of the mutant IA-2 allele by Southern blot analysis and PCR. All protocols were approved by our institutional animal care and use committees.

Genotyping. Tail DNA-PCR using four primers was designed to discriminate between wild-type (IA-$2^{+/+}$), heterozygous (IA-$2^{+/-}$), and homozygous (IA-$2^{-/-}$) mice. The wild-type allele was detected as a 1.3-kb product using an exon 3 sense primer (5′-TACAAGGTGTGCTCCGGCAACTCATGT-3′) and an exon 4 antisense primer (5′-GGTCCATCTCCTGGGAGATCACATGCT-3′). The recombinant allele was detected as a 3.5-kb product using the PGK-1 primer (5′-GGTGCTGTCCATCTGCACGAGACTAGT-3′) in the promoter of the neo cassette and an exon 7 antisense primer (5′-CAGCAGTCAATCTCTGCA GACTCAATT-3′). PCR was performed with the TaqPlus Precision PCR System (Stratagene) at 35 cycles of 94°C for 0.5 min, 60°C for 1 min, and 72°C for 3 min in a GeneAmp PCR System 9700 (Applied Biosystems, Forest City, CA). Each PCR product was separated on 1% agarose gels containing ethidium bromide and visualized under ultraviolet light.

RNA analysis. Total RNA from brain (10-week-old male IA-$2^{+/+}$, IA-$2^{+/-}$, and IA-$2^{-/-}$ mice) was isolated using TRIZOL reagent (Life Technology, Rockville, MD). For Northern blot analysis, 20 μg of each sample were separated on a 1% (wt/vol) agarose/2.2 mol/l formaldehyde gel and transferred to a Hybond-XL membrane (Amersham Pharmacia Biotech, Piscataway, NJ). The blot was subsequently hybridized with ^{32}P-radiolabeled mouse IA-2 cDNA intracellular and extracellular probes and an IA-2β cDNA 3′ noncoding region probe.

Western blot analysis. Brain samples from IA-$2^{+/+}$ or IA-$2^{-/-}$ mice were homogenized with PBS. After centrifugation at 10,000*g* for 5 min, cell debris was sonicated in lysis buffer (50 mmol/l Tris-HCl [pH 7.4], 150 mmol/l NaCl, 1 mmol/l EDTA, 1% sodium deoxycholate, 1% NP-40, 0.4% SDS, and 1 mmol/l phenylmethylsulfonyl fluoride). Equivalent amounts of protein dissolved in SDS-PAGE sample buffer were subjected to SDS-PAGE on an 8% polyacrylamide gel. Separated proteins were transferred onto polyvinylidine difluoride membranes by electrotransfer. Blots were processed as recommended by the manufacturer (enhanced chemiluminescence detection; Amersham Pharmacia Biotech). Rabbit anti−IA-2 serum made from the intracellular domain of recombinant mouse IA-2 and absorbed with brain lysate from IA-$2^{-/-}$ mice was used as the primary antibody (1:2,000 dilution) followed by anti-rabbit Ig antibody conjugated to horseradish peroxidase (Amersham Pharmacia Biotech).

Histological and immunohistochemical analysis. All the major organs and tissues were collected in 10% neutral-buffer formalin or 4% paraformaldehyde and processed for paraffin embedding. Sections were stained with hematoxylin and eosin. Pancreatic sections were incubated with antibodies to insulin, glucagon, or somatostatin (DAKO, Carpinteria, CA) followed by biotin-conjugated second antibody and streptavidin-horseradish peroxidase.

Intraperitoneal glucose tolerance test and insulin release. Mice aged 10–23 weeks were fasted for 16 h, followed by glucose injection (2 g/kg body wt i.p.). Venous blood was drawn from the tail vein at 0, 15, 30, 60, and 120 min after the injection. Blood glucose was measured using a portable glucometer (Bayer, Elkhart, IN). For acute insulin release, glucose (3 g/kg body wt) was injected intraperitoneally into male and female mice aged 10–23 weeks. Venous blood was collected at 0, 3, 9, and 15 min in heparinized tubes. After centrifugation, plasma was stored in −20°C. Insulin levels were measured with an enzyme-linked immunosorbent assay (ELISA) kit using a mouse insulin standard (ALPCO, Windham, NH).

Isolation of pancreatic islets. IA-$2^{-/-}$ or IA-$2^{+/+}$ mice were anesthetized with ketamine and xylazine. Pancreases were perfused with 3 ml of collagenase IV (2 mg/ml in Hank's solution; Life Technologies) and further digested in a water bath at 37°C for 25 min. The digested pancreases were washed with Hank's solution three times and passed through mesh to remove undigested tissues. The islet preparation was further subjected to percoll density gradient separation (density 1.089–1.062) and handpicked under a stereomicroscope (21). The purity of islets reached >95% and was verified by dithizone staining (22). The purified islets were cultured overnight in RPMI-1640 medium supplemented with 5.5 mmol/l glucose, 100 units/ml benzypenicillin, 100 μg/ml streptomycin, and 10% fetal bovine serum before insulin secretion tests.

Glucose-stimulated insulin secretion of pancreatic islets. Insulin secretion was measured by placing 10 islets in each of five wells (New Transwell Clear; Costar Scientific, Cambridge, MA). Experiments were repeated at least three times. The islets were preincubated in 1 ml oxygenated Krebs-Ringer bicarbonate buffer (KRBB) containing 143.5 mmol/l Na^+, 5.8 mmol/l K^+, 2.5 mmol/l Ca^{2+}, 25 mmol/l HCO_3, 0.3% BSA (Fraction V; ICN, Lisle, IL), and 3.3 mmol/l glucose at 37°C for 30 min. After preincubation, the islets were incubated in 1.0 ml of KRBB supplemented with 3.3 mmol/l glucose for 1 h. Subsequently, the islets were transferred to media containing 27.7 mmol/l glucose and incubated for 1 h. Aliquots were removed and stored at −20°C for quantitation of insulin by ELISA.

Statistical analysis. Statistical analysis was performed using the Student's *t* test for unpaired comparisons. Data are presented as means + SE. $P < 0.05$ was considered significant.

RESULTS

ES cells were transfected with the IA-2 targeting vector pPNT-IA-2 (Fig. 1). By homologous recombination of the targeting vector with the IA-2 wild-type locus, the 5′-upstream promoter region, exons 1–3 and introns 1, 2, and most 3 of the wild-type IA-2 locus were replaced with a neomycin cassette. Successful homologous recombination in ES cells was detected by Southern blot analysis of neomycin-resistant colonies with a 1.1-kb *Xho*I-*Hin*dIII fragment (outside probe) and a 1.9-kb neo probe (data not shown). Three IA-$2^{+/-}$ ES cells clones were injected into blastocysts to make chimeric mice that transmitted the modified IA-2 allele to their offspring. Wild-type (IA-$2^{+/+}$), heterozygous (IA-$2^{+/-}$), and homozygous (IA-$2^{-/-}$) mice were identified by tail DNA PCR with appropriate primers. As seen in Fig. 2*A*, wild-type IA-$2^{+/+}$ mice were identified by a 1.3-kb PCR product; homozygous IA-$2^{-/-}$ mice, by a 3.5-kb PCR product; and heterozygous IA-$2^{+/-}$ mice, by both 1.3- and 3.5-kb PCR products. The identification of these mice was confirmed by Southern blot analysis. As seen in Fig. 2*B*, tail DNA digested with *Kpn*I and hybridized with the 1.1-kb *Xho*I-*Hin*dIII outside probe produced a 6.9-kb band with IA-$2^{+/+}$ DNA, a 10.7-kb band with IA-$2^{-/-}$ DNA, and both a 6.9- and 10.7-kb band with IA-$2^{+/-}$ DNA.

Further evidence that the homologous recombination was successful and disrupted the IA-2 gene was obtained from Northern blot analysis. As seen in Fig. 2*C*, hybridization of total brain RNA with a probe corresponding to the extracellular domain of IA-2 (nt 485–1,708) resulted in a strong 3.8-kb band with IA-$2^{+/+}$ RNA, a marked reduction in the band with IA-$2^{+/-}$ RNA, and no band with IA-$2^{-/-}$ RNA. A probe corresponding to the intracellular domain of IA-2 (nt 1992–3036) yielded similar results (Fig. 2*D*). In contrast, a probe generated from the 3′ noncoding region (nt 3,040–3,193) of the closely related protein IA-2β (23,24) showed that IA-2β mRNA was not affected by the

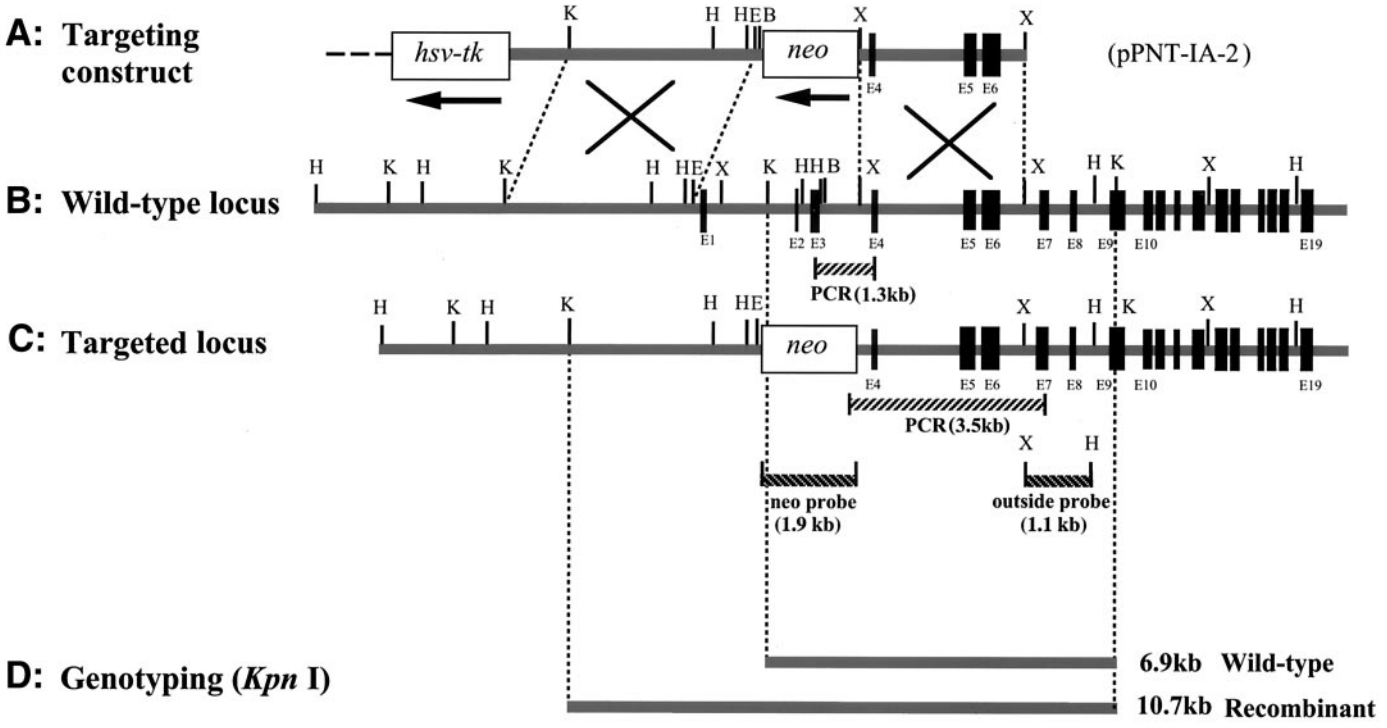

FIG. 1. Targeted disruption of the IA-2 gene. Vertical bars represent exons E1 through E19. Restriction enzyme sites shown are *Kpn*I (K), *Hin*dIII (H), *Eco*RI (E), *Xho*I (X), and *Bam*HI (B). *A*: Targeting construct shows that a portion of the 5′-upstream promoter, exons 1, 2, and 3 and introns 1, 2, and most of 3, are replaced by the neomycin cassette. *B*: Wild-type locus. Dashed lines with large "X" show areas where homologous recombination takes place. *C*: Targeted locus shows integration of targeting construct, containing the neomycin cassette, into the wild-type locus. *D*: Size of restriction fragments when wild-type locus and targeted locus are cleaved with *Kpn*I and hybridized with the 1.1-kb outside probe. Location of PCR products and probes was with PCR (1.3 kb), PCR (3.5 kb), neo probe (1.9 kb), and outside probe (1.1 kb).

IA-2 knockout and was expressed equally in IA-$2^{+/+}$ and IA-$2^{-/-}$ mice (Fig. 2*E*). Western blot analysis, using rabbit anti–IA-2 sera to measure protein expression in mouse brain extract, showed no expression of IA-2 protein in IA-$2^{-/-}$ mice as compared to IA-$2^{+/+}$ mice (Fig. 2*F*).

Physical examination of the IA-$2^{-/-}$ mice revealed no gross abnormalities. Litter size (data not shown) and body weight did not differ from the IA-$2^{+/+}$ mice (Fig. 3*A*). Histological studies failed to reveal any abnormality in the neuroendocrine cells of the IA-$2^{-/-}$ mice, including pancreatic islets (Fig. 4*A*) and brain (Fig. 4*E* and *F*), nor were abnormalities found in any of the other organs or cell types examined. Immunohistochemical studies on the IA-$2^{-/-}$ mice also revealed normal-appearing pancreatic islets, with no difference in the morphology or staining pattern of the insulin-, glucagon-, or somatostatin-producing cells (Fig. 4*B–D*) as compared to the IA-$2^{+/+}$ controls (not shown).

Nonfasting blood glucose levels of the IA-$2^{-/-}$ male mice, measured over a 22-week period, were slightly elevated as compared to IA-$2^{+/+}$ mice, but they did not fall within the diabetic range (Fig. 3*B*). Glucose tolerance tests, however, showed that glucose was significantly elevated at 15 and 30 min in both male and female IA-$2^{-/-}$ mice (Fig. 5*A*). Moreover, after glucose injection, acute insulin release was depressed in both male and female IA-$2^{-/-}$ mice, with statistically significant differences in the female mice and near significance ($P = 0.055$ at 15 min) in the male mice (Fig. 5B). In glucose-stimulated insulin secretion assays, pancreatic islets isolated from IA-$2^{-/-}$ mice also responded less vigorously to glucose stimulation. As seen in Fig. 6, male and female IA-$2^{-/-}$ mice released 48 and 42% less insulin, respectively, than IA-$2^{+/+}$ mice when switched from basal (3.3 mmol/l) to high (27.7 mmol/l) glucose.

DISCUSSION

Insulin is located in the dense-core secretory granules of pancreatic β-cells. Dense-core granules are complex structures, but a number of their constituents are now known (25). IA-2, a transmembrane glycoprotein, is an integral component of dense-core granules (16). The intracellular domain of IA-2 is thought to protrude into the cytoplasm of the cell, whereas at least a portion of the extracellular (luminal) domain resides within dense-core granules. There are two potential dibasic (KK) cleavage sites located at amino acid positions 386–387 and 448–449 of the extracellular domain. Transfection and pulse chase experiments have shown that IA-2 is expressed as a 120-kDa glycosylated protein that is then processed into a predominant 64-kDa fragment and several smaller fragments (26). Whether these fragments from the extracellular domain remain within the cytoplasm or are retained within the secretory granules is still not clear, nor is their function known. Similar posttranslational modifications have been observed in bovine pituitary cells (27). Except for these studies and a reported correlation between secretagogue stimulation of β-cells and upregulation of IA-2 mRNA (28,29), very little is known about the cell biology of IA-2.

In the present study, we succeeded in deleting the IA-2 gene by targeted gene disruption. Northern and Western

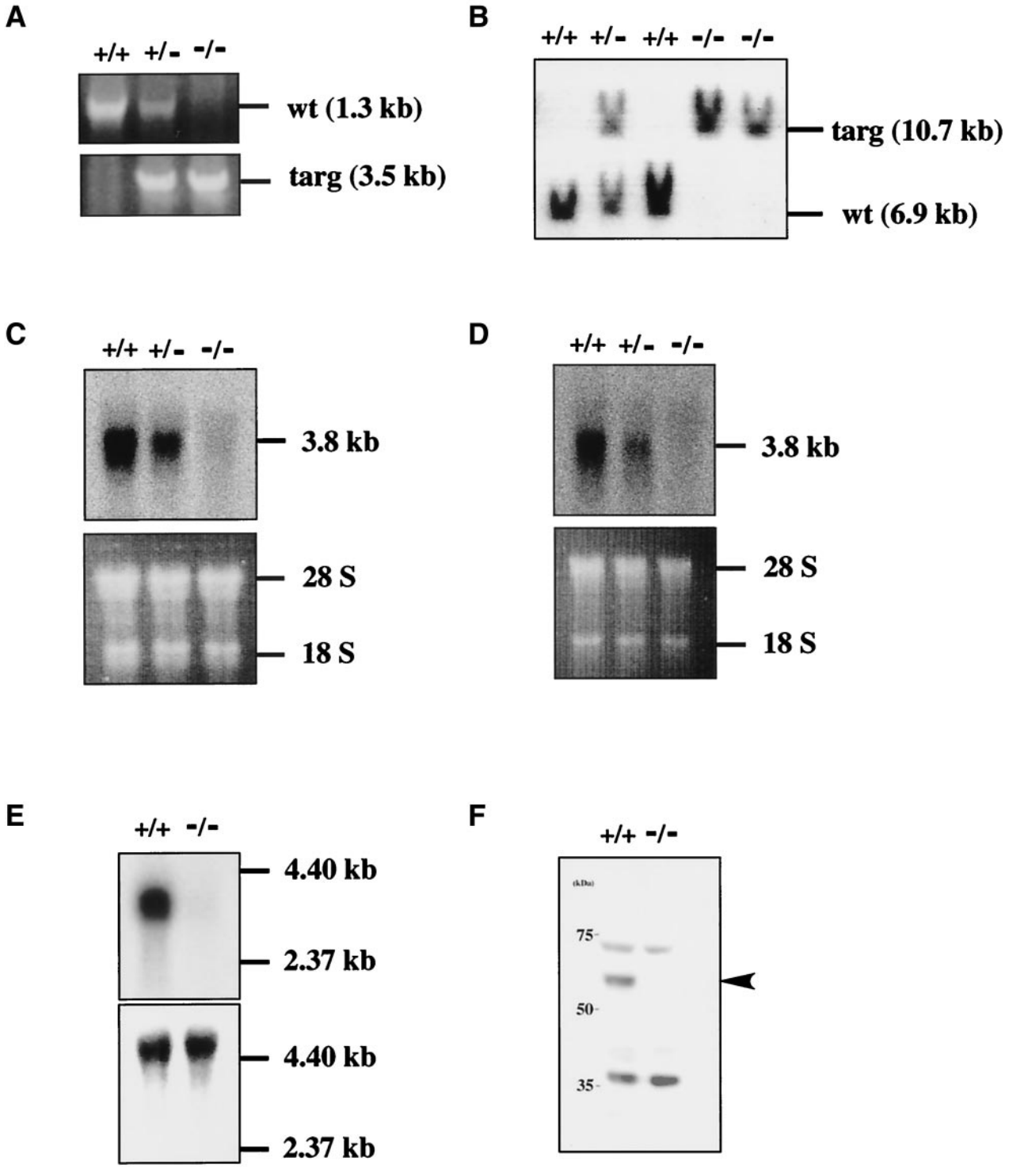

FIG. 2. Evidence for IA-2 gene disruption. *A*: PCR analysis. Primer pairs designed to produce a 1.3-kb product with cDNA from IA-2$^{+/+}$ mice, but a 3.5-kb product from IA-2$^{-/-}$ mice (see Fig. 1), showed that homologous recombination took place and that wild-type IA-2 had been eliminated. *B*: Southern blot analysis. DNA from IA-2$^{+/+}$, IA-2$^{+/-}$, and IA-2$^{-/-}$ mice were digested with *Kpn*I and hybridized with the 1.1-kb outside probe. DNA from the IA-2$^{+/+}$ mice yielded the expected 6.9-kb band, whereas DNA from the IA-2$^{-/-}$ mice gave a 10.7-kb band. IA-2$^{+/-}$ mice showed both bands. *C* and *D*: Northern analysis. Probes generated from either the extracellular (*C*) or intracellular (*D*) domains of IA-2 showed a strong 3.8-kb band with IA-2$^{+/+}$ mice, a weaker band with IA-2$^{+/-}$ mice, and no band with the IA-2$^{-/-}$ mice. *E*: IA-2β mRNA expression in IA-2$^{+/+}$ and IA-2$^{-/-}$ brain tissue. Probe generated from the intracellular domain of IA-2 showed a strong 3.8-kb band with IA-2$^{+/+}$, but no band with IA-2$^{-/-}$ mice (top). In contrast, a probe generated from the 3′ noncoding region of IA-2β showed a strong band (~5.5 kb) with both IA-2$^{+/+}$ and IA-2$^{-/-}$ mice (bottom). *F*: Western blot analysis. Antibody to IA-2 recognizes the IA-2 protein (arrow) in brain tissue from the IA-2$^{+/+}$ mice, but not from the IA-2$^{-/-}$ mice.

blot analysis showed that neither IA-2 mRNA nor protein was expressed. Although nonfasting blood glucose levels remained in the normal range, glucose tolerance tests revealed statistically significant elevated blood glucose levels in both male and female IA-2$^{-/-}$ mice. Glucose-stimulated insulin secretion showed statistically depressed insulin release in female IA-2$^{-/-}$ mice, with a similar trend, just missing statistical significance, in male

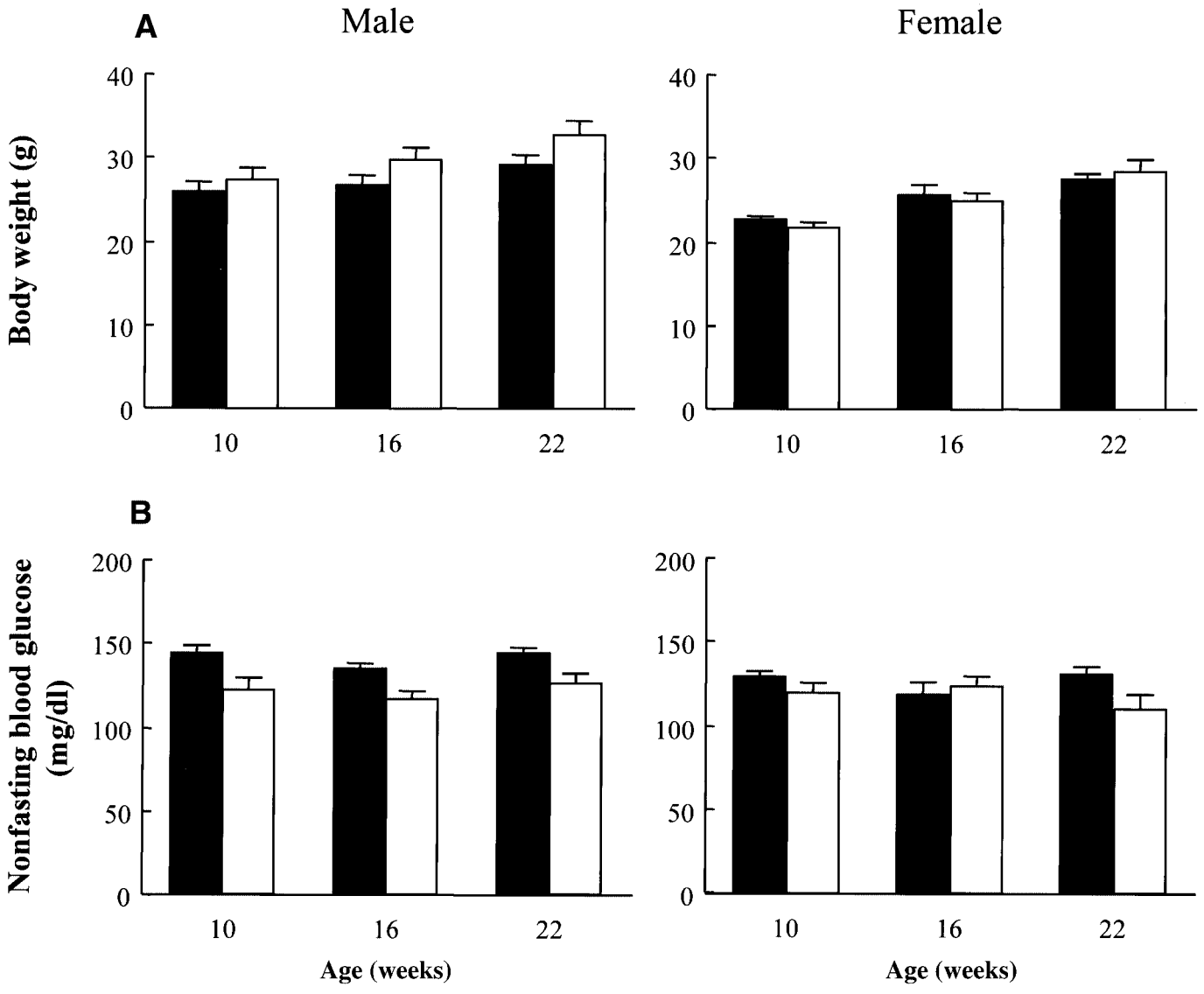

FIG. 3. Body weight and nonfasting blood glucose levels. Body weight (*A*) and nonfasting blood glucose levels (*B*) in male ($n = 6$) and female ($n = 6$) IA-2$^{-/-}$ (■) and male ($n = 6$) and female ($n = 6$) IA-2$^{+/+}$ (□) mice measured over 22 weeks. Data are means ± SE

IA-2$^{-/-}$ mice. Islets from both male and female IA-2$^{-/-}$ mice also showed significantly lower insulin release than islets from IA-2$^{+/+}$ mice when the cultures were switched from basal (3.3 mmol/l) to high (27.7 mmol/l) glucose levels. These findings, taken together with the known location of IA-2 in dense-core secretory granules, argue that IA-2 plays a role in insulin secretion. Although the alterations in glucose tolerance tests and insulin release are statistically significant, they are mild, and this may explain why IA-2$^{-/-}$ mice do not develop elevated nonfasting blood glucose levels and overt diabetes.

The findings with IA-2$^{-/-}$ mice raise questions about the contribution of IA-2β, also known as phogrin, to the secretory process. IA-2β is structurally similar to IA-2, showing 74% identity within the intracellular domain. This protein also is an integral component of dense-core granules and is phosphorylated in a Ca^{2+}-sensitive manner in response to secretagogue stimulation of β-cells (30). It is therefore possible that IA-2 and IA-2β work together or that one serves in a compensatory capacity for the other. However, at least at the mRNA level, IA-2 knockout does not result in a compensatory increase in IA-2β mRNA (Fig. 2*E*). Recently we succeeded in deleting the IA-2β gene (A.K. and A.L.N., unpublished data), and experiments are now underway to determine whether this protein also is involved in insulin secretion.

In terms of the pathogenesis of type 1 diabetes, it is of interest to ask whether there is any relationship between the autoimmune response to IA-2 and the functional role of IA-2 in secretion. It is known that autoantibodies to IA-2 are directed exclusively to the intracellular domain of the molecule that protrudes into the cytoplasm. Because there is no evidence that these autoantibodies are internalized and act within the cytoplasm, it seems unlikely that the autoimmune response to IA-2 would have any effect on the secretory function of the IA-2 molecule. Depressed insulin secretion, however, is one of the features of type 2 diabetes. Although

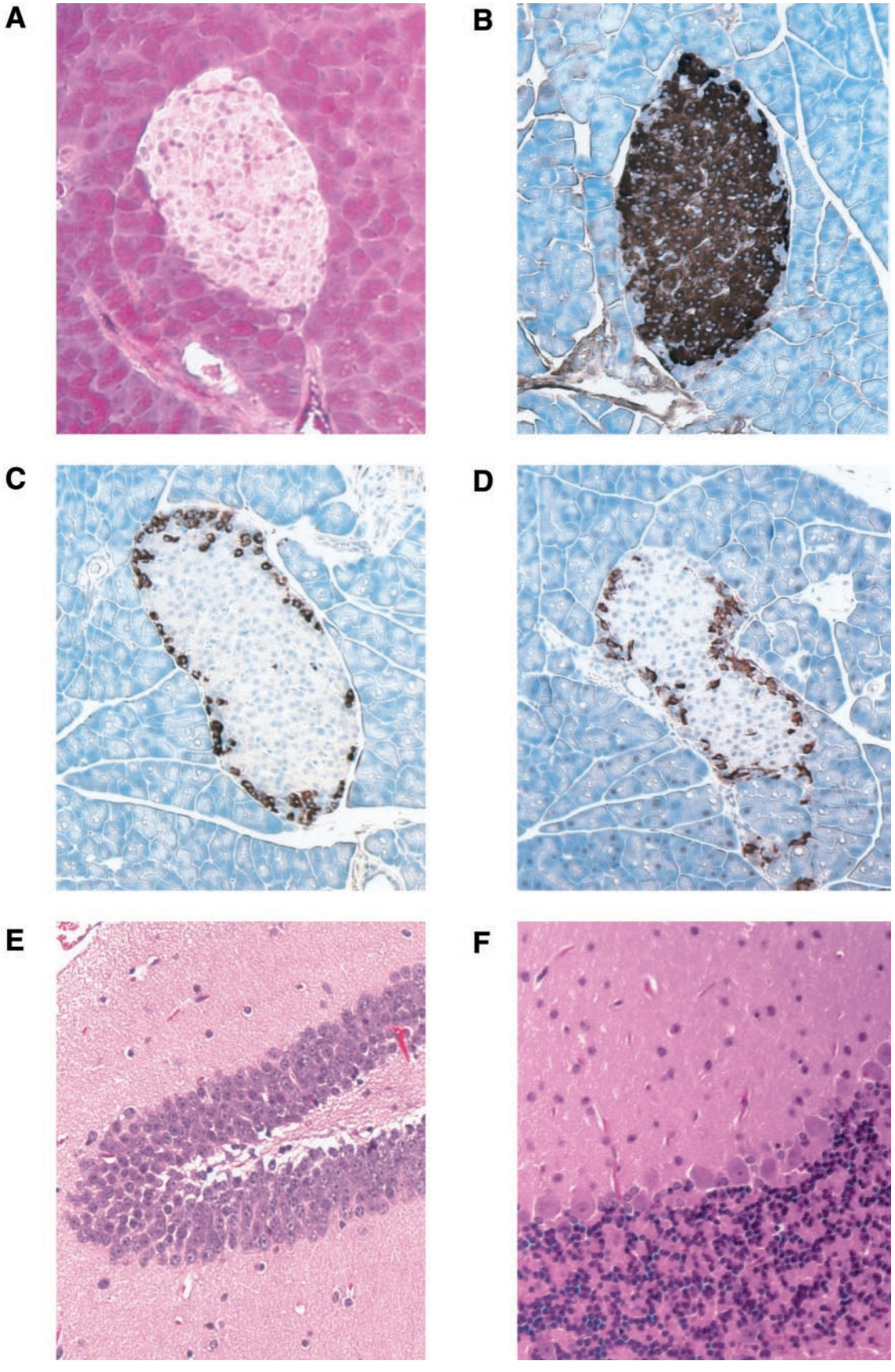

FIG. 4. Histological appearance and immunostaining of pancreases and brain from IA-2$^{-/-}$ mice. Sections of pancreases were fixed and stained with hematoxylin and eosin (*A*) or incubated with anti-insulin antibody (*B*), anti-glucagon antibody (*C*), or anti-somatostatin antibody (*D*) followed by biotin-conjugated second antibody and streptavidin horseradish peroxidase. Sections of brain (hippocampus [*E*] and cerebellum [*F*]) were fixed and stained with hematoxylin and eosin (magnification ×200 [*A*–*E*] and ×300 [*F*]).

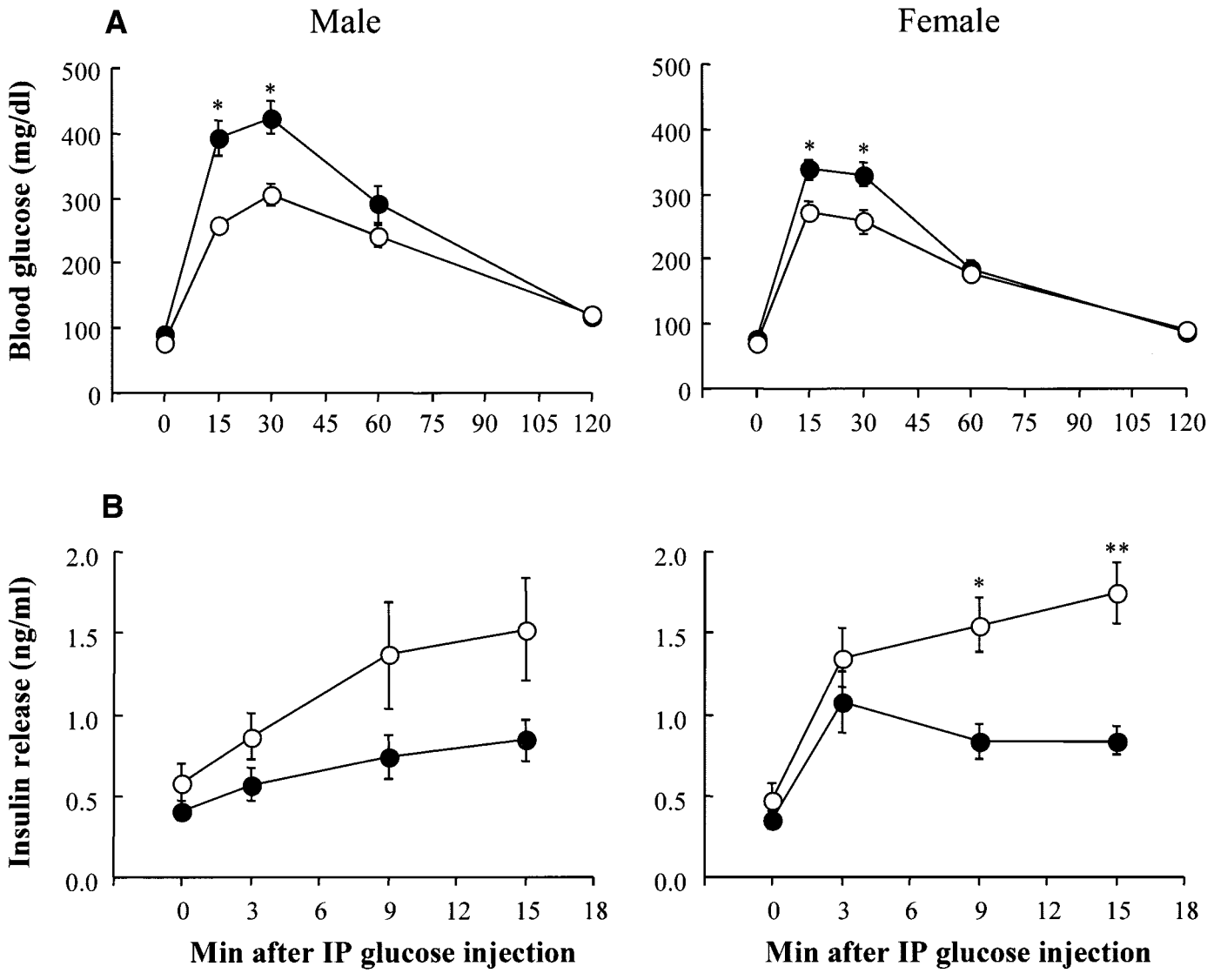

FIG. 5. Glucose tolerance and insulin secretion tests. *A*: Intraperitoneal (IP) glucose tolerance tests in male (n = 20) and female (n = 22) IA-2$^{+/+}$ (○) and male (n = 15) and female (n = 19) IA-2$^{-/-}$ (●) mice. After overnight fasting, D-glucose (2 g/kg body wt) was injected intraperitoneally, and blood glucose levels were measured at different time points. *B*: Acute insulin secretion in response to intraperitoneal glucose in male (n = 17) and female (n = 17) IA-2$^{+/+}$ (○) and male (n = 17) and female (n = 14) IA-2$^{-/-}$ (●) mice. Blood samples were drawn from the tail vein using heparinized capillary tubes before and after glucose injection (3 g/kg body wt). The results represent the average of three independent experiments. Data are means ± SE. *P < 0.01; **P < 0.001.

no association between IA-2 and type 2 diabetes has been recognized thus far, any gene that is involved in insulin secretion becomes a possible candidate gene for type 2 diabetes.

The process of secretion is complex and encompasses a number of different signals and pathways (25). Secretory vesicles are transported from the Golgi to the plasma membrane, where docking, priming, and fusion take place. Insulin is then secreted by exocytosis, a process that involves Ca^{2+} influx through voltage-dependent channels and regulation of exocytosis by a variety of phosphorylation events (31). Where in this multistep process IA-2 plays a role is not known. Recently, by use of the yeast two-hybrid system and co-immunoprecipitation, several proteins have been identified that bind to IA-2. This includes βIV spectrin and the PDZ domains of β2-syntrophin and neuronal nitric oxide synthase. Solimena and colleagues (32,33) have postulated that IA-2 may link the secretory granules with the actin cystoskeleton through its association with βIV spectrin or β2-syntrophin, and that this might affect granule traffic and exocytosis. Alternatively, because nitric oxide regulates the release of certain hormones, it is possible that the association of IA-2 with nitric oxide synthase may modulate insulin secretion.

The demonstration in the present study that deletion of IA-2 affects insulin secretion and the identification in other studies of IA-2 binding proteins (32,33) begin to provide insight into the function and possible mechanism of action of IA-2. The fact that IA-2 is present in the secretory granules of many different neuroendocrine cells raises the possibility that IA-2 may be involved not only in the secretion of insulin from β-cells, but also in the secretion of hormones from a broad range of neuroendocrine cells.

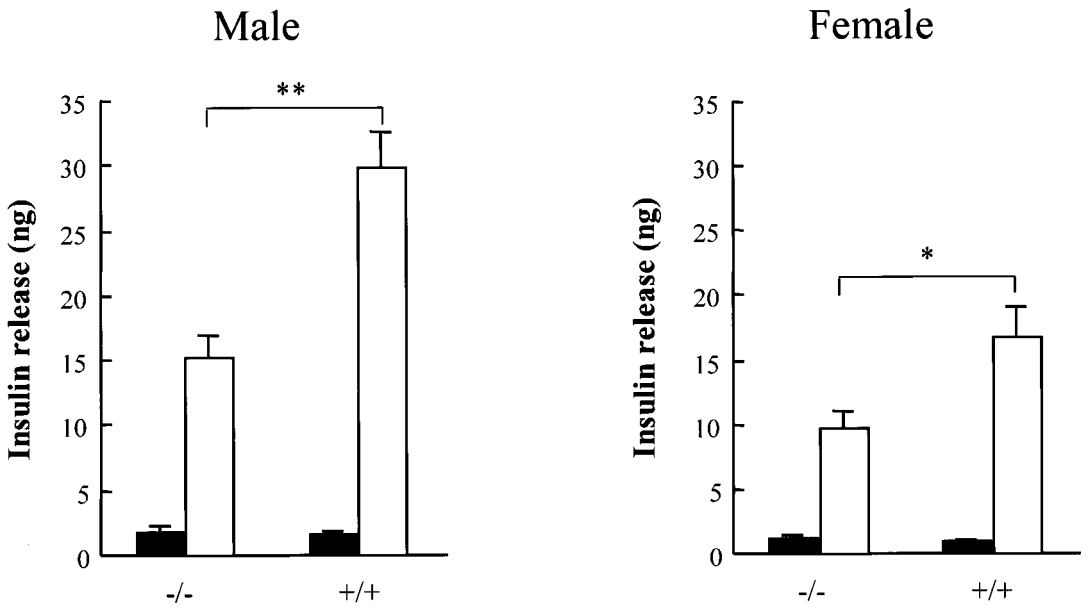

FIG. 6. Glucose-stimulated insulin release in vitro. Pancreatic islets isolated from IA-2$^{+/+}$ and IA-2$^{-/-}$ mice were placed in five wells, each containing 10 islets, in KRBB with 3.3 mmol/l glucose (■). At the end of 1 h, insulin levels in the supernatants were measured. The cells were then transferred to KRBB containing 27.7 mmol/l glucose (□), and at the end of 1 h insulin levels were again measured. The results represent the average of three independent experiments. Data are means ± SE. *P < 0.01; **P < 0.001.

ACKNOWLEDGMENTS

The authors thank Dr. Ashok Kulkarni for his advice and Glenn Longenecker for his help in preparing the IA-2 knockout mice.

REFERENCES

1. Lan MS, Lu J, Goto Y, Notkins AL: Molecular cloning and identification of a receptor-type protein tyrosine phosphatase, IA-2, from human insulinoma. *DNA Cell Biol* 13:505–514, 1994
2. Lan MS, Wasserfall C, Maclaren NK, Notkins AL: IA-2, a transmembrane protein of the protein tyrosine phosphatase family, is a major autoantigen in insulin-dependent diabetes mellitus. *Proc Natl Acad Sci U S A* 93:6367–6370, 1996
3. Gorus FK: Diabetes registries and early biological markers of insulin-dependent diabetes mellitus: Belgian Diabetes Registry. *Diabetes Metab Rev* 13:247–274, 1997
4. Verge CF, Gianani R, Kawasaki E, Yu L, Pietropaolo M, Jackson RA, Chase HP, Eisenbarth GS: Prediction of type I diabetes in first-degree relatives using a combination of insulin, GAD, and ICA512bdc/IA-2 autoantibodies. *Diabetes* 45:926–933, 1996
5. Hawa M, Rowe R, Lan MS, Notkins AL, Pozzilli P, Christie MR, Leslie RD: Value of antibodies to islet protein tyrosine phosphatase-like molecule in predicting type 1 diabetes. *Diabetes* 46:1270–1275, 1997
6. Bingley PJ, Bonifacio E, Williams AJ, Genovese S, Bottazzo GF, Gale EA: Prediction of IDDM in the general population: strategies based on combinations of autoantibody markers. *Diabetes* 46:1701–1710, 1997
7. Kulmala P, Savola K, Petersen JS, Vahasalo P, Karjalainen J, Lopponen T, Dyrberg T, Akerblom HK, Knip M: Prediction of insulin-dependent diabetes mellitus in siblings of children with diabetes: a population-based study: the Childhood Diabetes in Finland Study Group. *J Clin Invest* 101:327–336, 1998
8. Leslie RD, Atkinson MA, Notkins AL: Autoantigens IA-2 and GAD in type I (insulin-dependent) diabetes. *Diabetologia* 42:3–14, 1999
9. Notkins AL, Lernmark A: Autoimmune type I diabetes: resolved and unresolved issues. *J Clin Invest* 108:1247–1252, 2001
10. Lampasona V, Bearzatto M, Genovese S, Bosi E, Ferrari M, Bonifacio E: Autoantibodies in insulin-dependent diabetes recognize distinct cytoplasmic domains of the protein tyrosine phosphatase-like IA-2 autoantigen. *J Immunol* 157:2707–2711, 1996
11. Zhang B, Lan MS, Notkins AL: Autoantibodies to IA-2 in IDDM: location of major antigenic determinants. *Diabetes* 46:40–43, 1997
12. Xie H, Zhang B, Matsumoto Y, Li Q, Notkins AL, Lan MS: Autoantibodies to IA-2 and IA-2 beta in insulin-dependent diabetes mellitus recognize conformational epitopes: location of the 37- and 40-kDa fragments determined. *J Immunol* 159:3662–3667, 1997
13. Xie J, Zhang B, Lan MS, Notkins AL: Genomic structure and promoter sequence of the insulin-dependent diabetes mellitus autoantigen, IA-2 (PTPRN). *Genomics* 54:338–343, 1998
14. Cai T, Krause MW, Odenwald WF, Toyama R, Notkins AL: The IA-2 gene family: homologs in *Caenorhabditis elegans*, *Drosophila* and zebrafish. *Diabetologia* 44:81–88, 2001
15. Magistrelli G, Toma S, Isacchi A: Substitution of two variant residues in the protein tyrosine phosphatase-like PTP35/IA-2 sequence reconstitutes catalytic activity. *Biochem Biophys Res Commun* 227:581–588, 1996
16. Solimena M, Dirkx R Jr, Hermel JM, Pleasic-Williams S, Shapiro JA, Caron L, Rabin DU: ICA 512, an autoantigen of type I diabetes, is an intrinsic membrane protein of neurosecretory granules. *Embo J* 15: 2102–2114, 1996
17. Saeki K, Xie J, Notkins AL: Genomic structure of mouse IA-2: comparison with its human homologue. *Diabetologia* 43:1429–1434, 2000
18. Tybolewicz VL, Crawford CE, Jackson PK, Bronson RT, Mulligan RC: Neonatal lethality and lymphopenia in mice with a homozygous disruption of the c-abl proto-oncogene. *Cell* 65:1153–1163, 1991
19. Li E, Bestor TH, Jaenisch R: Targeted mutation of the DNA methyltransferase gene results in embryonic lethality. *Cell* 69:915–926, 1992
20. Geiser AG, Letterio JJ, Kulkarni AB, Karlsson S, Roberts AB, Sporn MB: Transforming growth factor beta 1 (TGF-beta 1) controls expression of major histocompatibility genes in the postnatal mouse: aberrant histocompatibility antigen expression in the pathogenesis of the TGF-beta 1 null mouse phenotype. *Proc Natl Acad Sci U S A* 90:9944–9948, 1993
21. Brunstedt J, Nielsen JH, Lernmark A, Hagedorn Study Group: Isolation of islets from mice and rats. In *Methods in Diabetes Research*. New York, John Wiley & Sons, 1985, p. 245–259
22. Latif ZA, Noel J, Alejandro R: A simple method of staining fresh and cultured islets. *Transplantation* 45:827–830, 1988
23. Lu J, Li Q, Xie H, Chen ZJ, Borovitskaya AE, Maclaren NK, Notkins AL, Lan MS: Identification of a second transmembrane protein tyrosine phosphatase, IA-2beta, as an autoantigen in insulin-dependent diabetes mellitus: precursor of the 37-kDa tryptic fragment. *Proc Natl Acad Sci U S A* 93:2307–2311, 1996
24. Wasmeier C, Hutton JC: Molecular cloning of phogrin, a protein-tyrosine phosphatase homologue localized to insulin secretory granule membranes. *J Biol Chem* 271:18161–18170, 1996
25. Lang J: Molecular mechanisms and regulation of insulin exocytosis as a paradigm of endocrine secretion. *Eur J Biochem* 259:3–17, 1999
26. Xie H, Deng YJ, Notkins AL, Lan MS: Expression, characterization,

processing and immunogenicity of an insulin-dependent diabetes mellitus autoantigen, IA-2, in Sf-9 cells. *Clin Exp Immunol* 113:367–372, 1998
27. Hermel JM, Dirkx R Jr, Solimena M: Post-translational modifications of ICA512, a receptor tyrosine phosphatase-like protein of secretory granules. *Eur J Neurosci* 11:2609–2620, 1999
28. Lee MS, Dirkx R Jr, Solimena M, Dannies PS: Stabilization of the receptor protein tyrosine phosphatase-like protein ICA512 in GH4C1 cells upon treatment with estriadol, insulin, and epidermal growth factor. *Endocrinology* 139:2727–2733, 1998
29. Seissler J, Nguyen TB, Aust G, Steinbrenner H, Scherbaum WA: Regulation of the diabetes-associated autoantigen IA-2 in INS-1 pancreatic beta-cells. *Diabetes* 49:1137–1141, 2000
30. Wasmeier C, Hutton JC: Secretatogue-dependent phosphorylation of the insulin granule membrane protein phogrin is mediated by cAMP-dependent protein kinase. *J Biol Chem* 276:31919–31928, 2001
31. Jones PM, Persaud SJ: Protein kinases, protein phosphorylation, and the regulation of insulin secretion from pancreatic beta-cells. *Endocr Rev* 19:429–461, 1998
32. Ort T, Maksimova E, Dirkx R, Kachinsky AM, Berghs S, Froehner SC, Solimena M: The receptor tyrosine phosphatase-like protein ICA512 binds the PDZ domains of beta2-syntrophin and nNOS in pancreatic beta-cells. *Eur J Cell Biol* 79:621–630, 2000
33. Berghs S, Aggujaro D, Dirkx R Jr, Maksimova E, Stabach P, Hermel JM, Zhang JP, Philbrick W, Slepnev V, Ort T, Solimena M: BetaIV spectrin, a new spectrin localized at axon initial segments and nodes of ranvier in the central and peripheral nervous system. *J Cell Biol* 151:985–1002, 2000